

A SIMULATION STUDY OF SINGLE CELL INSIDE AN INTEGRATED DUAL NANONEEDLE-MICROFLUIDIC SYSTEM

Muhammd Asraf Mansor, Mohd Ridzuan Ahmad*

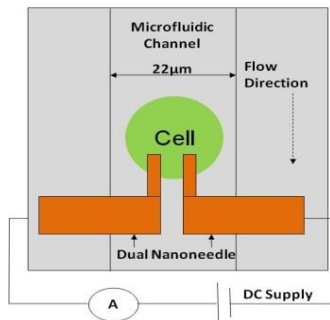
Micro-Nano System Engineering Research Group, Department of Control and Mechatronic Engineering, Universiti Teknologi Malaysia, 81310 UTM Johor Bahru, Malaysia

Article history

Received
30 October 2015
Received in revised form
15 February 2016
Accepted
28 March 2016

*Corresponding author
mdridzuan@utm.my

Graphical abstract



Abstract

Electrical properties of living cells have been proven to play significant roles in understanding of various biological activities including disease progression both at the cellular and molecular levels. Analyzing the cell's electrical states especially in single cell analysis (SCA) lead to differentiate between normal cell and cancer cell. This paper presents a simulation study of micro-channel and nanoneedle structure, fluid manipulation and current flow through HeLa cell inside a microfluidic channel. To perform electrical measurement, gold dual nanoneedle has been utilized. The simulation result revealed, the cell penetration occurs at microchannel dimension and solution flow rate is $22 \mu\text{m} \times 70 \mu\text{m} \times 25 \mu\text{m}$ (width x length x height) and 0.396 pL/min , respectively. The purposed device has capability to characterize the electrical property of single cells can be used as a novel method for cell viability detection in instantaneous manner.

Keywords: Dual nanoneedle, single cell analysis, finite element analysis, microfluidic

Abstrak

Sifat-sifat elektrik di dalam sel-sel hidup telah terbukti dalam memainkan peranan penting untuk memahami kepelbagaian aktiviti biologi termasuk perkembangan penyakit di peringkat selular dan molekul. Menganalisis sifat-sifat elektrik sel-sel hidup terutamanya sel tunggal, dapat membezakan antara sel normal dan sel kanser. Kertas kerja ini membentangkan kajian simulasi terhadap saluran mikro dan ciri-ciri jarum di dalam nano saiz, manipulasi cecair dan aliran semasa cecair dengan menggunakan sel HeLa di dalam saluran micro. Dwi nano jarum emas telah digunakan untuk tujuan pelaksanaan pengukuran elektrik. Hasil simulasi ini menunjukkan, penembusan ke dalam sel berlaku pada keadaan dimensi saluran mikro ialah $22 \mu\text{m} \times 70 \mu\text{m} \times 25 \mu\text{m}$ (lebar x panjang x tinggi) dan aliran cecair ialah 0.396 pL/min . Peranti ini mempunyai kebolehpayaan untuk mengukur sifat-sifat elektrik di dalam sel-sel tunggal dan boleh dijadikan sebagai kaedah baru untuk mengesan kebolehidupan sesuatu sel secara serta-merta.

Kata kunci: Dwi nano jarum emas, analisis sel tunggal, analisis elemen terhad, *microfluidic*

© 2016 Penerbit UTM Press. All rights reserved

1.0 INTRODUCTION

Study of cell has emerged as a distinct new field, and acknowledged to be one of the fundamental building blocks of life. Moreover, cells have unique biophysical and biochemical properties to maintain and sense the physiological surrounding environment

to fulfill its specific functions [1, 2]. Biophysical properties of cells provide early signals of disease or abnormal condition to the human body, which make them valuable as potential markers for identifying cancers [3-5], bacteria [6, 7], toxin detection [8] and the status of tissues [9, 10]. The conventional method for analyzing cell conductivity is done by population

based study [11]. However, the heterogeneity of the cells may lead inaccurate measurement when perform population based technique because each cell have unique biochemical and biophysical properties [12]. For that reason, single cell analysis (SCA) has been emphasized to provide biologists and scientists to peer into the molecular machinery of individual cells. In addition, in depth analysis, more fully described activities of cell differentiation and cancer can only be accomplished with single cell analysis [13], thus helps doctors to develop a prognosis and design a treatment plan for particular patients.

Electrical properties of cells provide some insight and vital information to aid the understanding of complex physiological states of the cell. Cells that experience abnormalities or are infected by bacteria may have altered ion channel activity [14], cytoplasm conductivity and resistance [15] and deformability [16]. Since electrical properties of cells have several advantages in cells analysis, many techniques has been reported to measure electrical parameter of single cell such as patch clamp [17], nanoprobes [18], electrorotation [19, 20], microelectrical impedance spectroscopy (μ -EIS) [21, 22] and impedance flow cytometry [23, 24]. The comparison of single cell electrical properties technique can be found in other articles [25, 26].

This study presents development of integrated dual nanoneedle-microfluidic device in the microfluidic finite element model for single cell analysis. In this paper, we perform the simulation of the microchannel and nanoneedle structure, fluid manipulation and current flow through HeLa cell by using finite element analysis software (Abaqus 6.14).

2.0 THE IDEA AND CONCEPT OF MODEL

The cytoplasm conductivity of cell can show the physiological state of the cell which is cancerous or healthy cell due to level of ions concentrations [27] and permeability [28]. The alteration and the movements of K, Mg and Ca out of the cell causing the high permeability and increase the current flow inside cell. Cell penetration technique inside microfluidic channel is a novel technique for determine current value flow passing through the single cell cytoplasm. Our previous single cell penetration has been done experimentally by using dual nano-probes integrated with nano manipulator. The measurement is conducted inside an Environmental-Scanning Electron Microscopy (E-SEM) [29]. Figure 1 illustrates the schematic diagram of the proposed concept.

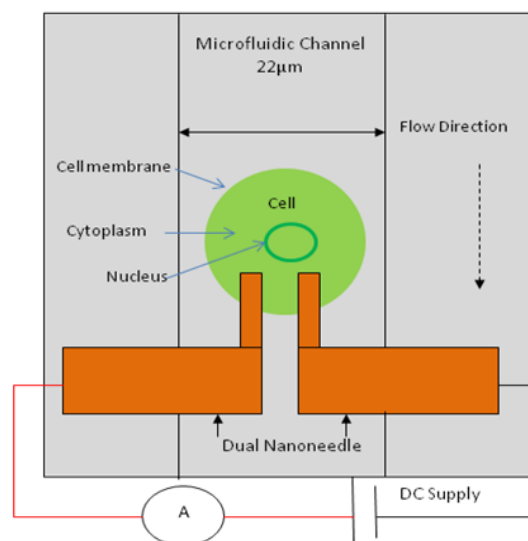


Figure 1 A schematic diagram of cell penetration inside microfluidic channel

The dual nanoneedle will be placed at a height half of microchannel. Cell will move toward dual nanoneedle by manipulating the fluid flow inside the microchannel. This manipulation will navigate the single cell to be penetrated by dual nanoneedle. When the penetration occurs, a small voltage (1V) will applied to the cell through conductive nanoneedle and the current flow across cell will be measured for analysis. A potential of 1 V was used so as to improve the reliability of the measured data [28]. In order to obtain a significant electrical characterization on single cells, the electrical measurement must be done at the intracellular area of the cell, i.e., cytoplasm, by penetrating a dual nanoneedle inside the cell. To prevent single cell bursting, only a short penetration will be performed. In this configuration, only the tip of the dual nanoneedle is in contact with the intracellular area the cell [30].

Several studies have reported that biological cells have a tendency to recover from small wounds [14]. Therefore, it is expected that the measured cells are still alive after being slightly penetrated by the dual nanoneedle. The size of the sample cell used in this experiment is 20 μ m diameters [31]. In order to prevent excessive damages to the cells during the penetration, the diameter of the nanoneedle's tip is in the range of 800 nm is used. Figure 2 shows the dimension of nanoneedle structure. The diameter of nanoneedle tips is 800 nm and length has been set to a penetration depth of less than 3 μ m. The tip diameter needs to be at least around ten times as small as the size of cells [32].

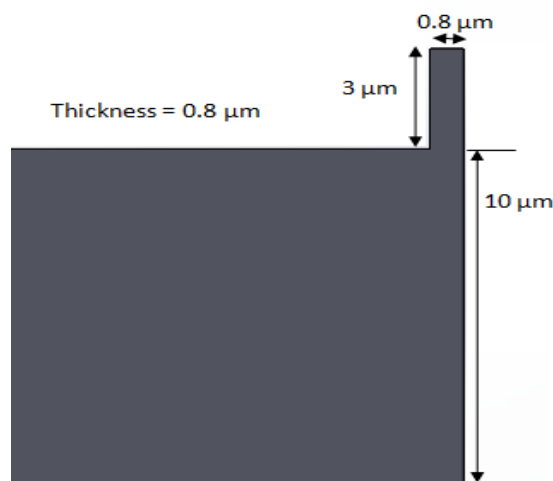


Figure 2 A model of a nanoneedle

3.0 SIMULATION

Simulation work is a significant process in every research area which has several advantages such as time constrain, minimize the cost, and safe [33]. In order to perform a realistic simulation, many parameters involved and one must be able to define the most relevance parameters as not all parameters are necessary to be acknowledged. In our simulation noisy and temperature were ignored because these parameter depend on the environment of the measurement. The microchannel dimension of this simulation is $22\ \mu\text{m} \times 70\ \mu\text{m} \times 25\ \mu\text{m}$ (width x length x height) with one inlet and one outlet. Finite element analysis software (Abaqus 6.14) which has the ability for multi-physics analysis was utilized to perform the simulation work.

3.1 Microchannel Optimization

Microchannel plays a major role in microfluidic device in order to perform an experiment related to microfluidic system. In our design, a dual nanoneedle was attached inside the microchannel. For that reason, the cross section area of the microchannel needs to be optimized. The purpose of microchannel optimization is to allow a single cell flow toward and touch a dual nanoneedle. The microchannel was modelled as 3D solid rigid combined with Eulerian water. Figure 3 illustrates the cross section of microchannel.

3.2 Mechanical Characteristic of Dual Nanoneedle

For mechanical characterization, the dual nanoneedle was modelled as 3D solid deformable and 6-node linear brick 3D stress element was used. Gold was utilized as a material of dual nanoneedle because it complies with our fabrication method (gold sputtering and electroplating technique). Density, and elastic properties of gold i.e. Young's

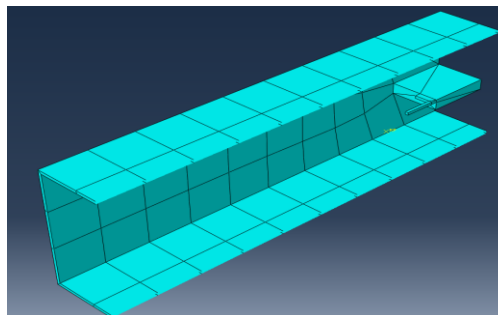


Figure 3 A cross section of microchannel structure

modulus, ultimate stress, present elongation and Poisson's ratio, were defined [34]. The model was meshed using hexahedron mesh type and both nanoneedle were encastred (fixed). Then the pressure was applied to the needle tip to measure the maximum force and to sustain the nanoneedle without broken. For rigidity of nanoneedle, aspect ratio (1:4) was used compare to our previous aspect ratio (1:10) [29]. Aspect ratio refers to the ratio between the diameter and length of the nanoneedle.

3.3 Flow Rate Optimization

Manipulation fluid flow rate inside the microfluidic channel is a significant role in single cell analysis. It is important to apply the appropriate flow rate in order to avoid excessive single cell penetration. Fluid flow rate in a microfluidic channel, Q can be calculated using equation (1):

$$Q = Av \quad (1)$$

where A is the cross section area of a channel and v is the fluid velocity. The unit for flow rate is litre per minute (l/min). The integrated dual nanoneedle-microfluidic device has a fixed channel cross section, thus only fluid velocity was manipulated in the optimization process through simulation.

The velocity is considered sufficient if the penetration process between dual nanoneedle and single cell is succeeded without excessive damage to the cell. In this simulation the flow rate is being controlled by applying initial velocity for fluid.

3.4 Electrical Measurement

Single cell electrical measurement was conducted during penetration process. In the electrical measurement, current flow through cell cytoplasm was being observed at two different conditions of electrode gap. The penetration depth is around $2\ \mu\text{m}$ depth. In this simulation, the current flow through the cells is represented by Electric Current Density (ECD). Current, I is obtained by using equation (2):

$$I = ECD \times A \quad (2)$$

where A is the cross-section area of cell. The type of element for the dual nanoneedle in this simulation was modelled as 3D solid deformable DC3D4E and a 4-node linear coupled thermal-electrical element. Figure 4 illustrates the simulation setup for single cell electrical measurement. The HeLa cell has been modelled as a spherical shape with a radius of 10 μm [31]. A potential of 1 V was applied to the right side nanoneedle and grounded on the left side.

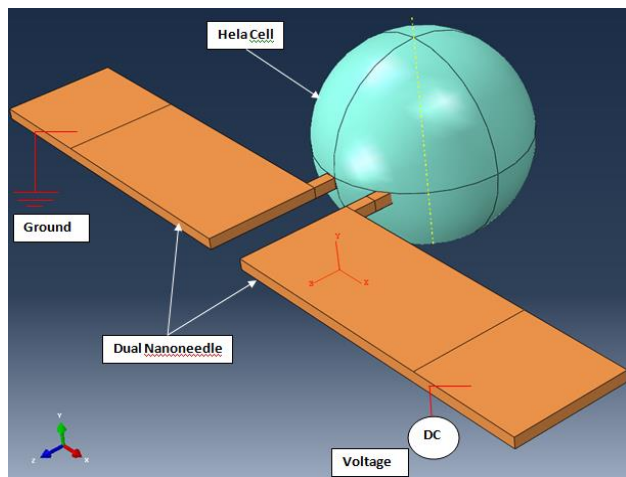


Figure 4 Single cell electrical measurement setup

4.0 RESULTS AND DISCUSSIONS

4.1 Microchannel Optimization Result

For single cell analysis, microchannel needs to be designed smaller than the size of a single cell to allow only a single cell is flow in the detection area [35]. In our design, three microchannel structures were tested during the simulation process. Figure 5 shows the result of dimension of 20 μm x 70 μm x 20 μm (width x length x height). The single cell was unable to move close enough towards the dual nanoneedle. Based on the stream line of water, it shows that the water intends to flow to the bottom of dual nanoneedle. High pressure at top of dual nanoneedle pushes the single cell from moving forward. At dimension of 20 μm x 70 μm x 25 μm (width x length x height), the movement of single cell was not smooth (cell was stop moving for a second). This situation occurs because of friction between single cells with side wall of microchannel. The optimum microchannel dimension have been obtained from this simulation was 22 μm x 70 μm x 25 μm (width x length x height), where a single cell successfully touching the dual nanoneedle.

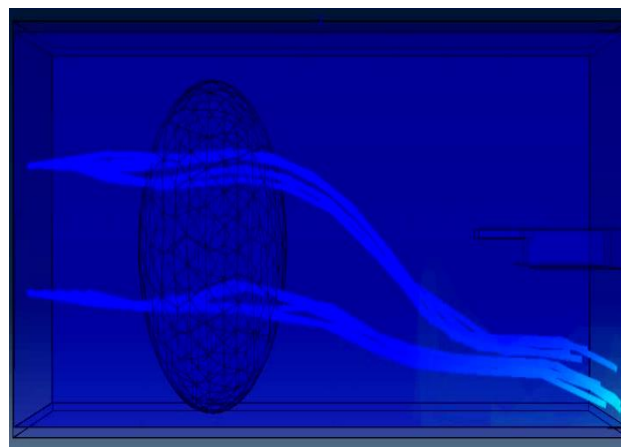


Figure 5 Stream line of water flow inside microchannel with dimension of 20 μm x 70 μm x 20 μm (width x length x height)

4.2 Dual Nanoneedle Mechanical Characteristic Result

In dual nanoneedle mechanical characteristic, validation was evaluated by comparison between simulation and calculation of maximum beam deflection. The maximum beam deflection, δ_{max} can be calculated by using equation (3):

$$\delta_{\text{max}} = PL^3/3EI \quad ; \quad I = wh^3/12 \quad (3)$$

where P is the applied force, E is the Young's Modulus, I is the area moment of inertia, and h, w, and L are the beam height, width, and length respectively. Young's Modulus for gold is 53 GPa [36]. Figure 6 shows the simulation result of tip displacement when 1 μN forces were applied. The highest displacement occurs at tip of nanoneedle by referring the colors indicator. From the simulation, the displacement of gold nanoneedle tip is 5.24 nm. Meanwhile the calculation of displacement tip is 4.975 nm. In term of value, simulation and calculation result show a high agreement.

In addition, the dual nanoneedle will receive impact force due to the momentum of a moving single cell. For this reason, nanoneedle damage factor also being investigated during the simulation process.

Figure 7 illustrates the dual nanoneedle was broken after applied force at 17 μN . From the investigations, the maximum force can be exerted to nanoneedle before its damaged is less than 17 μN . These results are comparable to reported penetration force of 1 μN for human epidermal melanocytes that is the only cell membrane without cell wall structure [37].

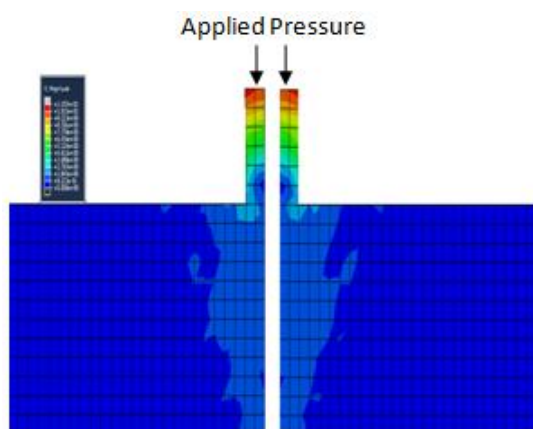


Figure 6 Nanoneedle tip displacement for applied force $1\mu\text{N}$

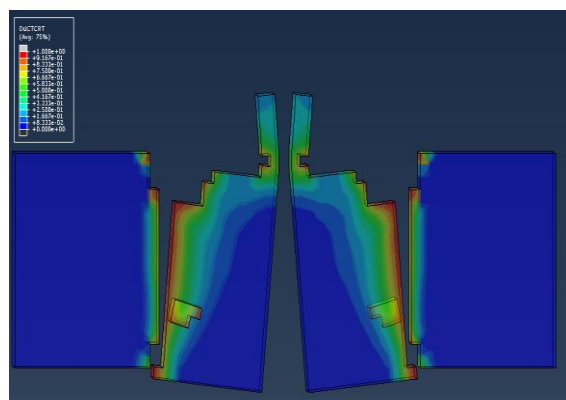


Figure 7 A damage of dual nanoneedle

4.3 Single Cell Penetration Result

Fluid rate of Deionised water (DI water) in microchannel has being analysis in this simulation in order to obtain the sufficient flow rate value for single cell penetration. The flow rate was controlled by applying velocity for fluid. The velocity will remain constant until the cell has been penetrated by the dual nanoneedle without excessive damage to the cell. At velocity of $0.5\ \mu\text{m/s}$ which is equivalent to a flow rate of $0.165\ \text{pL/min}$, the dual nanoneedle was unable to penetrate the single cell. The increment of $0.2\ \mu\text{m/s}$ from previous was used for another process. The dual nanoneedle was able to penetrate the single cell, however the penetration process need a waiting period off 3 second before penetrated. Then the velocity was increased to $1\ \mu\text{m/s}$ which is equivalent to a flow rate of $0.33\ \text{pL/min}$. At this velocity, the dual nanoneedle successfully penetrated the single cell without excessive damage to the cell. In order to find the maximum limit of flow rate, the velocity was increased at $0.2\ \mu\text{m/s}$ increment from previous value. Based on analysis, at velocity of $1.4\ \mu\text{m/s}$, the single cell was experienced excessive penetration, thus it cause damage to the cell. Table 1 shows the summary of a fluid flow rate optimization result.

Table 1 A fluid flow rate optimization result

No.	Velocity, $\mu\text{m/s}$	Flow Rate, pL/min	Penetration
1	0.5	0.165	No
2	0.7	0.231	Yes (Need Time)
3	1.0	0.33	Yes
4	1.2	0.396	Yes
5	1.4	0.462	Yes (Excessive)

4.4 Single Cell Electrical Measurement Result

The electrical measurement on single cells using the dual nanoneedle was done after the dual nanoneedle penetrating the cytoplasm of cell. Figure 8 shows the electrical measurement of HeLa cell. Once the tip of dual nanoneedle was inside cytoplasm of cell, 1-V potential voltage was applied. The output current flow through the cells was obtained by using equation (2). The simulation has been carried out for two different gap distances of dual nanoneedle, which is possible to fabricate inside microfluidic device by using photolithography, sputtering and electroplating technique.

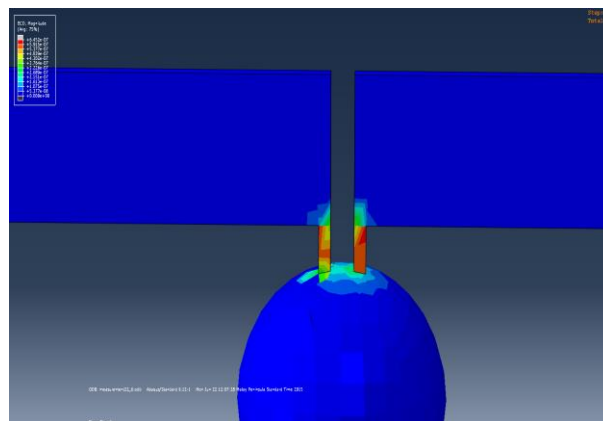


Figure 8 Electrical measurement of single cell

Table 2 shows the electric current density (ECD) and current flow of HeLa cell. The current flow inside cytoplasm of HeLa cell in this simulation was $46.4\ \text{nA}$ for gap distance between electrode is $2\ \mu\text{m}$. The reported HeLa cell current measurement by using patch clamp technique is around 40 to $50\ \text{nA}$ [38].

Table 2 Result of ECD and current for HeLa cell at different nanoneedle gap

No.	Gap Distance (μm)	HeLa Cell	
		ECD (A/m^2)	Current (nA)
1	2	36.924	46.4
2	4	40.823	51.3

5.0 CONCLUSION

This study presents a simulation of microfluidic device integrated with dual nanoneedle that can perform physical penetration and measurement of current flow inside as single cell. The result shows a promising functional sensor in application of medical research for evaluation or investigation of cancer cell at single cell level. Furthermore, the ability to characterize the electrical property of single cells can be used as a novel method for cell viability detection in instantaneous manners.

Acknowledgement

This work was supported by grants from the Ministry of Education Malaysia (grant No. 4L640 and 4F351) and Universiti Teknologi Malaysia (grant No. 02G46, 03H82 and 03H80).

References

- [1] J. El-Ali, P. K. Sorger, and K. F. Jensen. 2006. Cells on Chips. *Nature*. 442(710): 403-41.
- [2] S. Suresh, J. Spatz, J. P. Mills, a Micoulet, M. Dao, C. T. Lim, M. Beil, and T. Seufferlein. 2005. Connections between Single-Cell Biomechanics and Human Disease States: Gastrointestinal Cancer and Malaria. *Acta Biomaterialia*. 1(1): 15-30.
- [3] H. M. Coley, F. H. Labeed, H. Thomas, and M. P. Hughes. 2007. Biophysical Characterization of MDR Breast Cancer Cell Lines Reveals the Cytoplasm is Critical in Determining Drug Sensitivity. *Biochimica et Biophysica Acta*. 1770(4): 601-608.
- [4] Y. Cho, A. B. Frazier, Z. G. Chen, and A. Han. 2009. Whole-Cell Impedance Analysis for Highly and Poorly Metastatic Cancer Cells. *Journal of Microelectromechanical Systems*. 18(4): 808-817.
- [5] Y. Zhao, D. Chen, Y. Luo, H. Li, B. Deng, S.-B. Huang, T.-K. Chiu, M.-H. Wu, R. Long, H. Hu, X. Zhao, W. Yue, J. Wang, and J. Chen. 2013. A Microfluidic System for Cell Type Classification Based on Cellular Size-Independent Electrical Properties. *Lab on a Chip*. 13(12): 2272-2277.
- [6] S. M. Radke and E. C. Alocilja. 2005. A High Density Microelectrode Array Biosensor for Detection of E. coli O157:H7. *Biosensors and Bioelectronics*. 20(8): 1662-1667.
- [7] E. Du, S. Ha, M. Diez-Silva, M. Dao, S. Suresh, and A. P. Chandrakasan. 2013. Electric Impedance Microflow Cytometry for Characterization of Cell Disease States. *Lab on a Chip*. 13(19): 3903-3909.
- [8] F. Asphahani and M. Zhang. 2007. Cellular Impedance Biosensors for Drug Screening and Toxin Detection. *Analyst*. 132(9): 835-841.
- [9] C. Gabriel, S. Gabriel, and E. Corthout. 1996. The Dielectric Properties of Biological Tissues: I. *Literature Survey*. 41: 2231-2249.
- [10] M. R. Stoneman, M. Kosempa, W. D. Gregory, C. W. Gregory, J. J. Marx, W. Mikkelsen, J. Tjoe, and V. Raicu. 2007. Correction of Electrode Polarization Contributions to the Dielectric Properties of Normal and Cancerous Breast Tissues at Audio/Radio Frequencies. *Physics in Medicine and Biology*. 52(22): 6589-6604.
- [11] D. Das, F. A. Kamil, K. Biswas, and S. Das. 2014. Evaluation of Single Cell Electrical Parameters from Bioimpedance of a Cell Suspension. *RSC Advances*. 4(35): 18178.
- [12] T. A. Nguyen, T. Yin, D. Reyes, and G. A. Urban. 2013. Microfluidic Chip with Integrated Electrical Cell-Impedance Sensing for Monitoring Single Cancer Cell Migration in Three-Dimensional Matrixes. *Analytical Chemistry*. 85(22): 11068-11076.
- [13] B. F. Brehm-Stecher and E. A. Johnson. 2004. Single-Cell Microbiology: Tools, Technologies, and Applications. *Microbiology and Molecular Biology Reviews*. 68(3): 538-559.
- [14] K. Kunzelmann. 2005. Ion Channels and Cancer. *Journal of Membrane Biology*. 205(3): 159-173.
- [15] S.-B. Huang, Y. Zhao, D. Chen, H.-C. Lee, Y. Luo, T.-K. Chiu, J. Wang, J. Chen, and M.-H. Wu. 2014. A Clogging-Free Microfluidic Platform with an Incorporated Pneumatically Driven Membrane-Based Active Valve Enabling Specific Membrane Capacitance and Cytoplasm Conductivity Characterization of Single Cells. *Sensors and Actuators B: Chemical*. 190: 928-936.
- [16] M. Abdolahad, Z. Sanaee, M. Janmaleki, S. Mohajerzadeh, M. Abdollahi, and M. Mehran. 2012. Vertically Aligned Multiwall-Carbon Nanotubes to Preferentially Entrap Highly Metastatic Cancerous Cells. *Carbon*. 50(5): 2010-2017.
- [17] B. Sakmann and E. Neher. 1984. Patch Clamp Techniques for Studying Ionic Channels in Excitable Membranes. *Annual Review of Physiology*. 46: 455-472.
- [18] M. R. Ahmad and M. Nakajima. 2009. Single Cells Electrical Characterizations using Nanoprobe via ESEM-Nanomanipulator System. *IEEE Conference on Nanotechnology*. 8: 589-592.
- [19] J. Yang, Y. Huang, X. Wang, X. B. Wang, F. F. Becker, and P. R. Gascoyne. 1999. Dielectric Properties of Human Leukocyte Subpopulations Determined by Electrorotation as a Cell Separation Criterion. *Biophysical Journal*. 76(6): 3307-3314.
- [20] W. M. Arnold and U. Zimmermann. 1982. Rotating-Field-Induced Rotation and Measurement of the Membrane Capacitance of Single Mesophyll Cells of Avena Sativa Sites. *Zeitschrift für Naturforsch.* 37: 908-915.
- [21] A. Han and a B. Frazier. 2006. Ion Channel Characterization using Single Cell Impedance Spectroscopy. *Lab on a Chip*. 6(11): 1412-1414.
- [22] C. M. Kurz, H. Büth, A. Sossalla, V. Vermeersch, V. Toncheva, P. Dubruel, E. Schacht, and H. Thielecke. 2011. Chip-Based Impedance Measurement on Single Cells for Monitoring Sub-Toxic Effects on Cell Membranes. *Biosensors and Bioelectronics*. 26(8): 3405-3412.
- [23] S. Gawad, L. Schild, and P. H. Renaud. 2001. Micromachined Impedance Spectroscopy Flow Cytometer for Cell Analysis and Particle Sizing. *Lab on a Chip*. 1(1): 76-82.
- [24] N. Haandbæk, S. C. Bürgel, F. Heer, and A. Hierlemann. 2014. Characterization of Subcellular Morphology of Single Yeast Cells using High Frequency Microfluidic Impedance Cytometer. *Lab on a Chip*. 14: 369-377.
- [25] Y. Zheng, J. Nguyen, Y. Wei, and Y. Sun. 2013. Recent Advances in Microfluidic Techniques for Single-Cell Biophysical Characterization. *Lab on a Chip*. 13(13): 2464-2483.
- [26] M. A. Mansor and M. R. Ahmad. 2015. Single Cell Electrical Characterization Techniques. *International Journal of Molecular Sciences*. 16(6): 12686-12712.
- [27] S. Ingebrandt, G. Wrobel, S. Eick, S. Schafer, and A. Offenhausser. 2007. Probing the Adhesion and Viability of Individual Cells with Field-Effect Transistors. *International Solid-State Sensors, Actuators and Microsystems Conference*: 803-806.
- [28] R. K. Sahu, U. Zelig, M. Huleihel, N. Brosh, M. Talyshinsky, M. Ben-Harosh, S. Mordechai, and J. Kapelushnik. 2006. Continuous Monitoring of WBC (Biochemistry) in an Adult Leukemia Patient using Advanced FTIR-Spectroscopy. *Leukemia Research*. 30(6): 687-693.
- [29] M. R. Ahmad, M. Nakajima, M. Kojima, S. Kojima, M. Homma, and T. Fukuda. 2012. Instantaneous and

- Quantitative Single Cells Viability Determination using Dual Nanoprobe Inside ESEM. *IEEE Transactions on Nanotechnology*. 11(2): 298-306.
- [30] M. R. Ahmad, M. Nakajima, S. Kojima, M. Homma, and T. Fukuda. 2008. In Situ Single Cell Mechanics Characterization of Yeast Cells using Nanoneedles Inside Environmental SEM. *IEEE Transactions on Nanotechnology*. 7(5): 607-616.
- [31] M.-H. Wang and L.-S. Jang. 2009. A Systematic Investigation Into the Electrical Properties of Single HeLa Cells via Impedance Measurements and COMSOL Simulations. *Biosensors and Bioelectronics*. 24(9): 2830-2835.
- [32] Yajing Shen, M. Nakajima, M. R. Ahmad, T. Fukuda, S. Kojima, and M. Homma. 2009. Single Cell Penetration using Nano-Pipette by E-SEM Nanorobotic Manipulation System. *International Conference on Mechatronics and Automation*. 8: 1849-1854.
- [33] W. Fichtner. 2008. Overview of Technology Computer-Aided Design Tools and Applications in Technology Development, Manufacturing and Design. *Journal of Computational and Theoretical Nanoscience*. 5(6): 1089-1105.
- [34] J. M. Gere. 2001. *Mechanics of Materials*. 5th Edition. Brooks/Cole, New York.
- [35] Y. N. Luo, D. Y. Chen, Y. Zhao, C. Wei, X. T. Zhao, W. T. Yue, R. Long, J. B. Wang, and J. Chen. 2014. A Constriction Channel Based Microfluidic System Enabling Continuous Characterization of Cellular Instantaneous Young's Modulus. *Sensors and Actuators, B: Chemical*. 202: 1183-1189.
- [36] J. R. Greer, W. C. Oliver, and W. D. Nix. 2005. Size Dependence of Mechanical Properties of Gold at the Micron Scale in the Absence of Strain Gradients. *Acta Materialia*. 53(6): 1821-1830.
- [37] I. Obataya, C. Nakamura, S. Han, N. Nakamura, and J. Miyake. 2005. Nanoscale Operation of a Living Cell using an Atomic Force Microscope with a Nanoneedle. *Nano Letters*. 5(1): 27-30.
- [38] S. Li and L. Lin. 2007. A Single Cell Electrophysiological Analysis Device with Embedded Electrode. *Sensors and Actuators A: Physical*. 134(1): 20-26.